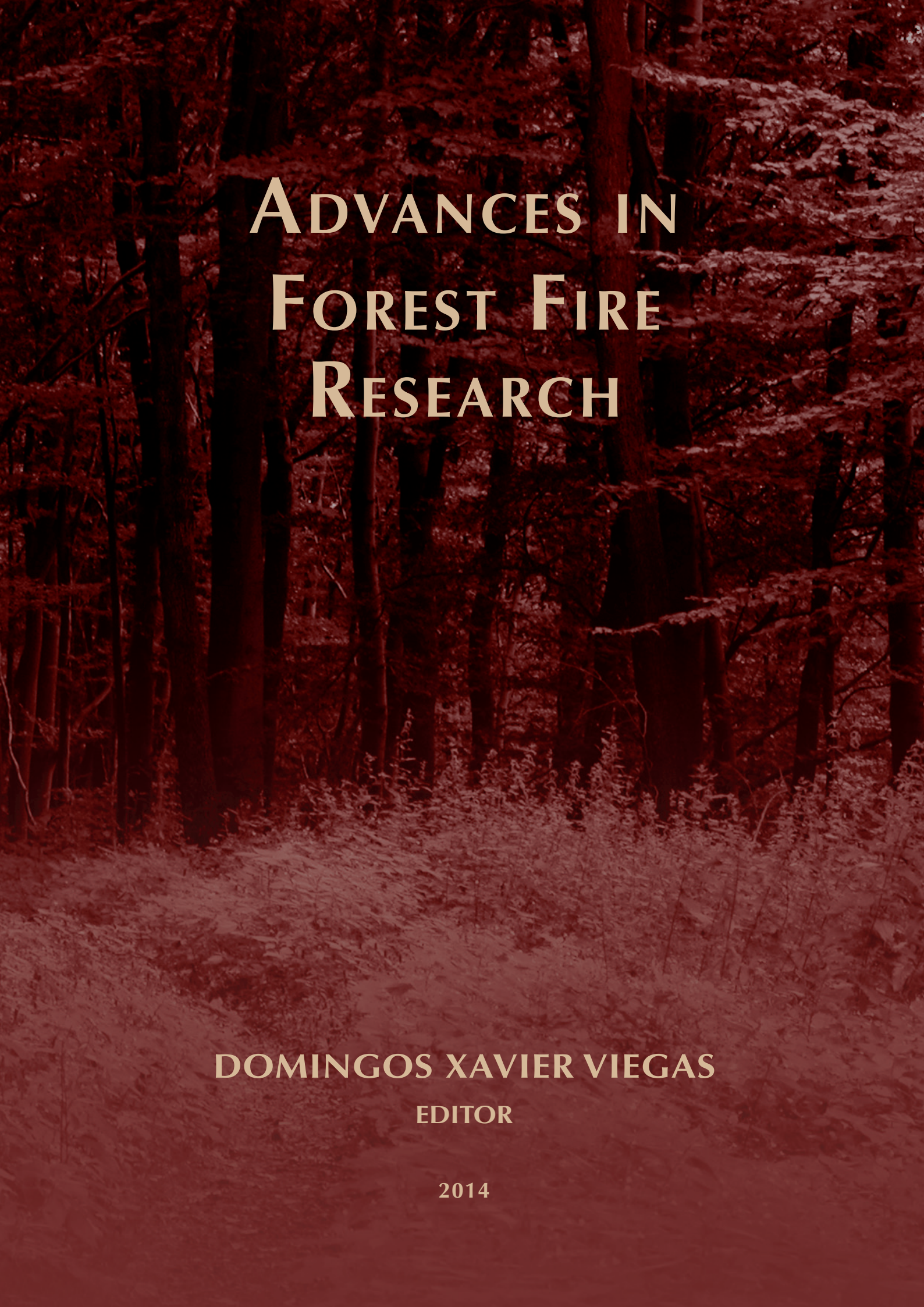

Advances in Forest Fire Research

DOMINGOS XAVIER VIEGAS

EDITOR

2014

Experimental and numerical study of fire behaviour: effects of the width on the rate of spread

Alexis Marchand, Nicolas Trevisan, Anthony Collin and Pascal Boulet

LEMTA, 2 Avenue de la Forêt de Haye TSA 60604 54518 Vandoeuvre-lès-Nancy cedex, alexis.marchand@univ-lorraine.fr

Abstract
This study focuses on the influence of the fuel bed width on the rate of spread. An experimental set-up based on visible cameras combined with image processing was used and a direct linear transformation (DLT) algorithm was developed in order to quantify fire propagation features such as the rate of spread, the fire length, ... The present work gathers results aimed at demonstrating the dependence of the rate of spread on the fire front morphology. A new cellular automaton was developed to better understand the heat transfer mechanisms, investigating in particular the role of radiative transfer.

***Keywords**: Fire propagation, cellular automaton model, Fire front width effect, Radiative transfer*

Glossary

HHV	Higher heating value [kW/kg]	Hf	Flame height [m]
LHV	Lower heating value [kW/kg]	RVR	Residual vegetation ratio [kg/kg]
RH	Relative humidity [%]	Cp_{dry}	Heat capacity [kJ/kg/K]
L	Fuel bed width [m]	F	View factor [-]
Lc	Distance from a point to the cylinder centre [m]	V_f	Flame volume [m^3]
		T_f	Flame temperature [K]
Rf	Flame radius	φ	Radiative heat flux [W]
z	Vertical coordinate [m]		

1. Introduction

Every year, several million hectares of vegetation are burnt by forest fires or bush fires, ravaging both flora and fauna. The knowledge of the fire behaviour is an important issue in order to prevent from disaster or to try to control the fire propagation. In this frame, the accurate estimation of the propagation rate is of major interest for the fire prevention.
It is commonly accepted that the rate of spread depends on the vegetation properties, the topography and the meteorological conditions. Some fire propagation codes, such as Farsite [1] and Behave [2], take these parameters into account when simulating the fire behaviour. However, these models are unable to include the real fire front morphology (fire length, shape ...) in their predictions. The rates of spread are evaluated only for linear fire fronts and can overpredict the fire propagation in many other configurations. Only physical models involving space varying terms in balance equations, namely in radiation or convection models, are really able to reproduce the real fire behaviour.
Fingering (burnt areas with small fire front widths) is an example of a non linear configuration in real fires. In 2001, pictures of real fires taken from satellite were analysed by Caldarelli [3], focusing on the fractal dimension and lacunarities observed in fires. Indeed satellite images show the existence of fingerings. At this scale, the fire propagation is affected by the fire front morphology, as it was already observed experimentally by Anderson in 1968 [4]. It is very important to model efficiently the fire behaviour at small scale (meter scale) in order to predict accurately the fire front evolution against time.

The aim of this contribution is to demonstrate through experimental data or numerical results that the rate of spread depends on the fuel bed width. Moreover this paper gives some issues to explain this phenomenon.
This contribution is divided as follows: Section 1 presents the platform PROMETHEI used to generate surface fires and the experimental data on the fire front. Section 2 details and analyzes the obtained experimental results. Section 3 presents the fire propagation model developed using the concept of cellular automaton. Section 4 proposes some comparisons between experimental and numerical results, giving some issues for a better understanding of the interaction between the fire front morphology and the rate of spread. Section 5 draws some conclusions and perspectives concerning this work.

2. Experimental set-up

Our experimental fire platform, named PROMETHEI, was used to provide a database on surface fires. This platform was built to better understand the fire behaviour and to calibrate or to validate the fire propagation model.
Experiments were carried out on a combustion table using excelsior as fuel bed (Figure 1). In order to observe different fire front morphologies, the fuel bed width was varied in the range between 25 cm to 3.5 m, the fire being ignited on a line along the whole bed width. In such configurations, the fire fronts are near-parabolic, but the front curvature varies with the line width and the rate of spread is also affected. The vegetation load was set at 0.5 kg/m².

Figure 1. Picture of surface fire front propagation

2.1. Image analysis

Pictures of the flame front during the fire propagation were taken with 4 visible cameras, 2 cameras for the back edge and 2 for the leading edge. Typical images are presented in grey-scale in Figure 2(a). The post-processing algorithm which was used, is based on an Otsu algorithm [5]. When this approach is applied, the flame volume is then clearly identified (Cf. Figure 2(b)). The leading edge and the back edge are then localized by two pixel swaps, horizontal and vertical crossing pixel method (Cf. Figure 2(c)). This method was repeated on all the pictures taken during the fire propagation.

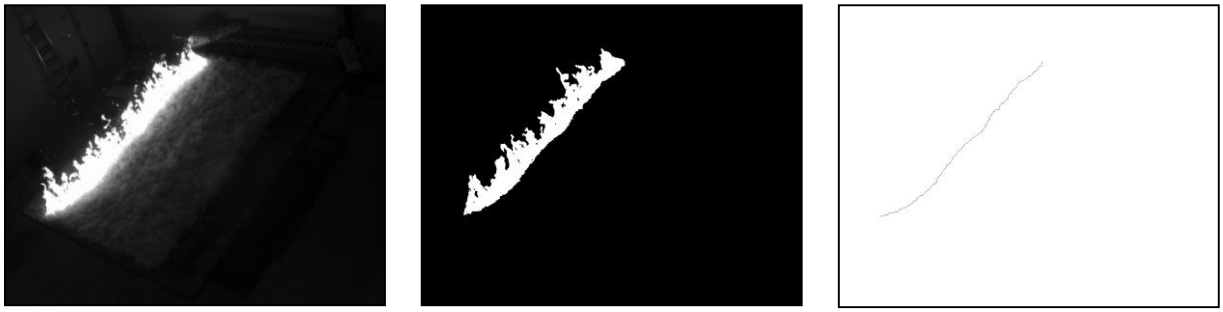

(a) (b) (c)

Figure 2. (a) Image in grey-scale obtained from one camera (b) Binary image after Otsu algorithm application (c) Detected fire front

2.2. Front reconstruction

The leading edge and the back edge were first localized on each picture, through pixel coordinates (Cf. Figure 2(c)). A direct linear transformation (DLT), method based on the work by Pastor *et al.* [6] was then applied on each pixel to merge the fire front in a real space in meter. Two examples of fire front detection are given in Figure 3(a) and Figure 3(b) for two different fuel bed widths (*L*).

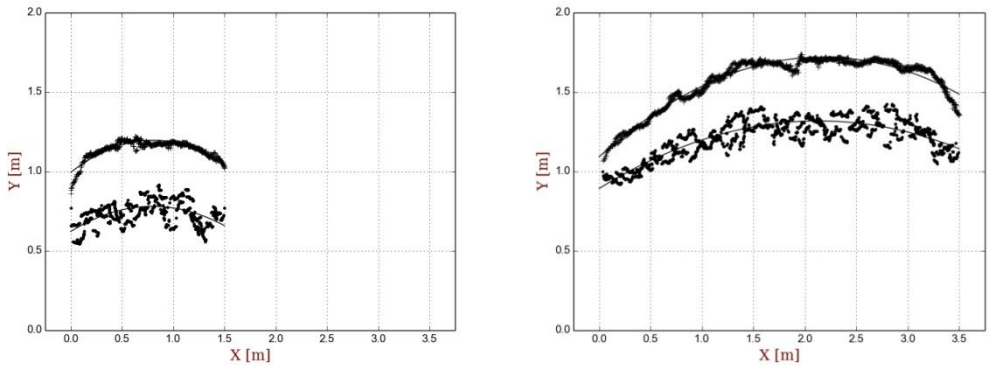

(a) ***(b)***

Figure 3. Fire front (top and back front) reconstructions after DLT algorithm (a) L = 1.5 m at t = 75.1 s after ignition (b) L = 3.5 m at t = 106.3 s after ignition

2.3. Repeatability and validation

In order to evaluate the accuracy of the image analysis, the results (in terms of rate of spread) provided by the Otsu-DLT algorithm were compared with the ones obtained using three other methods : (i) evaluation using chronometers (simple measurement of the distance with time of the most advanced point of the fire front) (v_{ch}), (ii) registration based on thermocouples (v_t), (iii) evaluation using dedicated photo-resistors (adapted from the work by Catchpole *et al.* [7]) (v_p). All these techniques were involved on the same experimental conditions, repeated 4 times. For the evaluations based on thermocouples and photo-resistors, the method consists in detecting a peak (of temperature or intensity) at several locations on the combustion table, allowing the estimation of the fire front location and then of the rate of spread. For this test, the experiment involved a fuel bed 2 m wide and 3 m long, with the vegetation load set at 0.5 kg/m². Results are gathered in Table 1.

The results obtained with the Otsu-DLT algorithm (v_{ca}) are first discussed. For the same experiment, the results vary in the range between 1.49 and 1.6 cm/s and the average rate of spread is estimated at 1.55 cm/s. The mean discrepancy is then evaluated at 2.7% which proves the good repeatability of the experimental device. Concerning the comparison with the other experimental methods, the mean

discrepancies are in the range from 1.7 to 4.6%. These small differences demonstrate the good accuracy of the Otsu-DLT algorithm involved in this work.

Table 1. Comparison of the different methods for rate of spread measurements [cm/s]

Experiment number	v_{ca}	v_{ch}	v_p	v_t	Mean discrepancies [%]
#1	1.6	1.51	1.45	1.63	4.6
#2	1.49	-	1.42	1.51	1.7
#3	1.53	1.49	1.45	1.50	3.4
#4	1.59	1.58	1.51	1.59	1.9

2.4. Environmental conditions

The physical properties (Lower Heating Value, Higher Heating Value, Residual Humidity, Residual Vegetation Ratio and Heat Capacity) of E*xcelsior* used in this study were characterized by the LERMAB laboratory, France. All these features are gathered in Table 2.

Table 2. Characteristics of the excelsior combustible

LHV [kW/kg]	HHV [kW/kg]	RH [%]	RVR [kg/kg]	Cp_{dry} [kJ/kg/K]
16180	20180	12.4	0.27	1430

In order to study the change in the rate of spread as a function of the fuel bed width, two series of experiments were carried out in different environmental conditions (see Table 3). For each experiment, relative humidity and temperature were given by a weather station. The environmental conditions were near constant during each experiment as it can be observed in Table 3.

Table 3. Environmental conditions

Width Fire [m]	Relative Humidity [%]	Temperature [°C]
0.25	64	6.1
0.5	66	6.4
0.75	67	6.9
1	67	6.8
1.5	70	6.7
2	69	6.7
2.5	69	7.0
3	68	6.7
3.5	70	6.8

(a) Experiment #1

Width Fire [m]	Relative Humidity [%]	Temperature [°C]
0.25	52	18.0
0.5	51	18.2
0.75	50	18.3
1	50	17.2
1.5	51	17.8
2	50	18.5
2.5	48	18.9
3	47	19.3
3.5	49	18.6

(b) Experiment #2

3. Results

3.1. Rate of spread

Figure 4 gives an example of results provided by the Otsu-DLT algorithm (for experiment #1 with a 3.5 m fuel bed width). The locations of the leading edge and the back edge were estimated as a function of time. The evolution is clearly linear, even at the first instants when the propagation starts. The rate of spread was deduced from the slope of the lines using a least squares method.

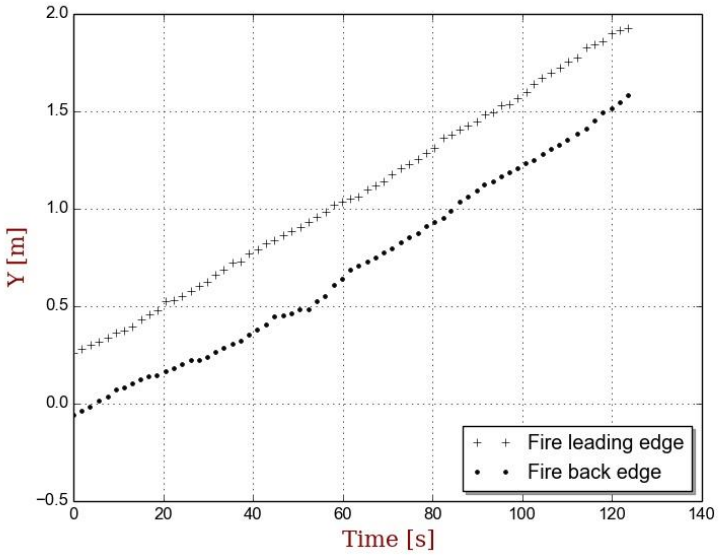

Figure 4. Example of fire front locations as a function of time, fire leading edge and back edge for a bed width L = 3.5 m

The evolution of the rate of spread (ROS) as a function of the fuel bed width is plotted in Figure 5 for Experiments #1 and #2. The ROS quickly increases for small fuel bed widths (between 25 cm to 100 cm) and reaches an asymptotic value above a 100 cm width. The limiting ROS is 1.6 cm/s for Experiment #1 and 1.3 cm/s for Experiment #2. As results tend to follow an exponential law, a fit of the ROS was sought for each experiment with the following relationship

$$ROS(L) = A_1\left(1 - exp\left(-A_2 L\right)\right)$$

The parameters A_1 and A_2 were estimated using a least squares method, yielding the following values:

- Experiment #1: A_1 = 1.28 cm/s and A_2 = 3.04 m^{-1}
- Experiment #2: A_1 = 1.62 cm/s and A_2 = 2.24 m^{-1}

The predictions based on these parameters are in good agreement with the experimental results as presented in Figure 5. A_2 parameter seems to be universal for this kind of experiment (for given vegetation and load) whereas A_1 parameter clearly depends on environmental conditions.

3.2. Fire thickness

The fire thickness was measured for the different experiments using the Otsu-DLT algorithm. For a given fire, the two fronts are interpolated with a second order polynomial, such as $Y(X) = aX^2 + bX + c$ (X and Y are the two coordinates associated with the combustion table). Such polynomial interpolations were presented in Fig 3(a) and Fig 3(b). The fronts were represented using

100 points equally spaced along the fire line. The thickness was then defined as the average distance between the two lines for a given *X* coordinate. Figure 6 gives the thickness evolution against the fire width. The fire thickness seems to be independent of the fire width. The average fire thickness is estimated at 33 cm (with average discrepancy of 7%) for Experiment #1 and at 24 cm for Experiment #2 (with average discrepancy of 4%). It can be observed that the ROS of Experiment #1 is slower than the one of Experiment #2, whereas its thickness is larger than the one of Experiment #2.

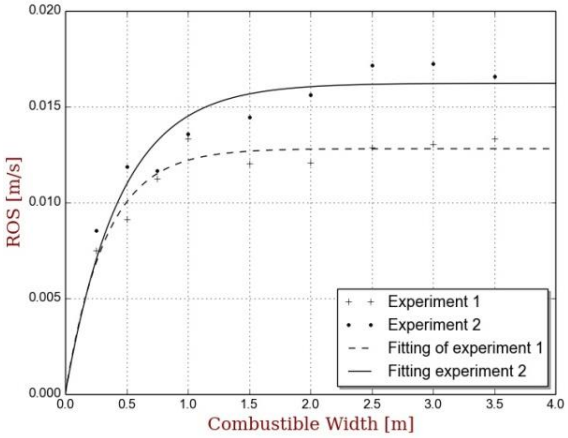

Figure 5. Evolution of the ROS with combustible width

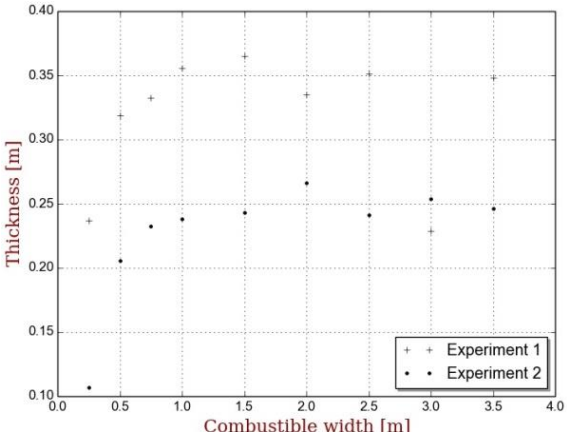

Figure 6. Evolution of the fire thickness with combustible width

3.3. Fire leading edge length

During the fire propagation, for a given time, the fire front is here modelled by a second order polynomial ($Y(X) = aX^2 + bX + c$). The total length of the fire front is then calculated as:

$$Length = \int_{Fire\ Front} ds = \frac{1}{4a}\left(Argsh(2aL+b) - Argsh(b) + (aL+b)\sqrt{(aL+b)^2} - b\sqrt{b^2+1} \right)$$

The evolution of the fire front total length against the fuel bed width is represented in Figure 7. The total length of the fire front is the same for the two experiments. Its evolution is linear with a slope close to 1 (accurate value equal to 1.02). The results demonstrate that the shape (or the length) of the fire front is independent of the environmental conditions.

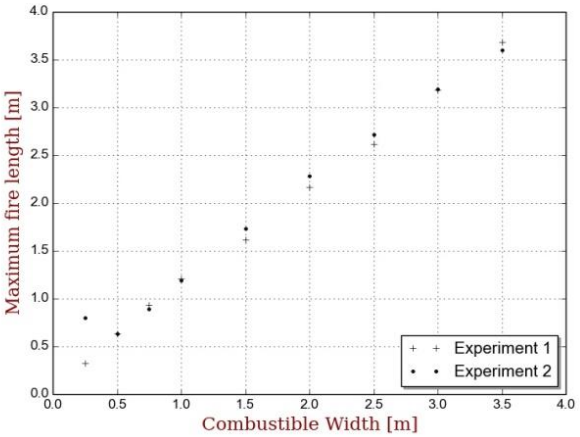

Figure 7. Evolution of the flame front length against the fuel bed width

4. Automaton model

4.1. Method

This model is based on the work by Porterie *et al.* [8]. The fuel bed is represented by a set of elementary hexagonal cells. The physical properties are assumed to be constant on the numerical domain. Radiation is supposed to be the main heat transfer involved in the fire propagation.

A cellular automaton model consists in associating a given state to each cell. The state of a cell is governed by a dimensionless time, τ. In the present work, the cells are described by one of these states:

(1) raw material ($\tau=0$) **(2)** heating ($0<\tau<\tau_d$)

(3) burning ($\tau_d<\tau<\tau_d+\tau_c$) **(4)** burned vegetation ($\tau_{d+}\tau_c<\tau$)

This kind of models requires a clear definition of the transition law between two states *i* and *j*, and the model parameters τ_d and τ_c. These transition laws can be experimentally defined or they can be extended from a physical model.

When the radiative transfer coming from the flame front is incident on the raw vegetation, the cell state switches from 1 to 2. The cell is heated due to the radiative transfer until a flame appears above the studied cell. At each iteration, an additional $\Delta\tau$ is associated to the characteristic time τ of the considered cell, with $\Delta\tau$ defined as,

$$\Delta\tau = A \sum_{Flame\ cell} \varphi_{Flame\rightarrow vegetation}$$

where *A* is a model parameter and $\sum_{Flame\ cell} \varphi_{Flame\rightarrow vegetation}$ is the total radiative contribution of the fire front toward the studied cell.

$\varphi_{Flame\rightarrow vegetation}$ is the radiative flux from one of the cells located on the fire front toward the "vegetation" cell. The flame is assumed to be represented by an equivalent cylinder with an absorption coefficient κ and a flame temperature T_f. The radiative contribution is evaluated thanks to a view factor calculation and $\varphi_{Flame\rightarrow vegetation}$ is defined by :

$$\varphi_{Flame\rightarrow vegetation} = 4\,F\,\kappa\,\sigma\,{T_f}^4\,V_f S_{cell}$$

V_f is the flame volume, S_{cell} the cell "vegetation" surface and *F* is the view factor evaluated as

$$F = \frac{1}{4\pi V_f}\sum_{\theta i}\left(g\left(Lc,R_f,H_f,\theta i\right) - g\left(Lc,R_f,0,\theta i\right) - g\left(Lc,0,H_f,\theta i\right) + g\left(Lc,0,0,\theta i\right)\right)\Delta\theta$$

where θi is discretized between 0 and 2π using a $\Delta\theta$ step. *Lc* is the distance between the burning cell and the "vegetation" cell. The *g* function is defined by

$$g\left(l,r,z,\theta\right) = \sqrt{l^2 - 2rl\cos\left(\theta\right) + r^2 + z^2} + l\cos\left(\theta\right)\ln\left(r - l\cos\left(\theta\right)\right) + \sqrt{l^2 - 2rl\cos\left(\theta\right) + r^2 + z^2}$$

The main advantage of this quasi-analytical relationship for *F* is to avoid the use of an accurate but time-consuming numerical method, such as a Monte Carlo Method to model the radiative transfer.

When τ is equal to τ_d (which represents the time of pyrolysis) the cell switches to state (3). It stays in state (3) during a time τ_c which describes the time during which the cell is burning. After burning, the state of cellular changes to (4).

Table 4. Cellular automaton model parameters

Edge of Hexagon [m]	Flame temperature T_f [K]	Absorption coefficient κ [1/m]	Flame height H_f [m]	$\tau_{d/A}$	τ_c
0.025	1733	0.1	0.4	50	13

The parameters used for the numerical study are gathered in Table 4. T_f, κ and H_f are identified using a PSO (Particle Swarm Optimization) algorithm with experimental data on radiative heat flux measured during a fire propagation test.

4.2. Numerical results and comparisons

Numerical simulations were done considering the fuel bed width in the range between 0.25 m and 4.0 m. Figure 8 gives two examples of fire propagations for fuel bed widths equal to 1.5 m and 3.5 m.
At this stage, the present model is able to capture some qualitative trends experimentally observed; in particular the model captures the parabolic shape of the fire fronts. These shapes must be compared with experimental measurements given in Figure 3 (a) and 3(b).

(a) ***1.5 m fuel bed width*** ***(b) 3.5 m fuel bed width***

Figure 8. Fire front spread simulated with the automaton model. Green: cellular in state (2) Orange: cellular in state (3) Brown: cellular in state (4) at 38th iteration.

One aim of the study was to show the ROS dependence on the bed width. As it was previously mentioned, the ROS depends on the environmental conditions, which are not directly involved in the present model. However, as it was observed in Figure 5, the ROS for the two experiments seem to follow the same trend. Hence, in order to compare the results, each rate of spread was divided by its asymptotic value. The corresponding evolution of the normalized ROS with the width is represented in Figure 9 (experimental fits and numerical values). The agreement is quite satisfactory. The evolution of the ROS with the fuel bed width is well described by the cellular automaton model, despite the fact that only the radiative transfer is considered in the heat transfer. Moreover, as the ROS does not vary for a fuel bed width above 1 m, this demonstrates that the radiative transfer coming from the fire front does not affect the vegetation which is located at a distance beyond 1 m. In other words, 1 m is the cut off distance for the radiative transfer in this kind of experiment.

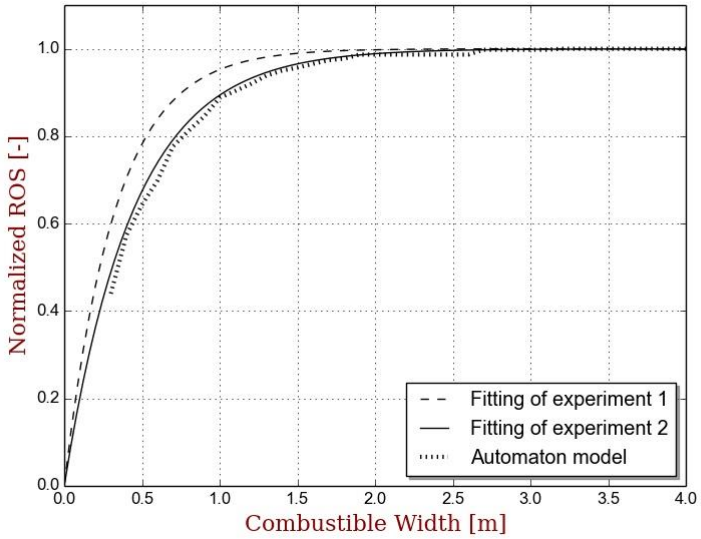

Figure 9. Normalized rate of spread for the two experiments and for the numerical model

5. Conclusion

A method based on image processing and direct linear transformation was used in order to reconstruct the leading edge and the back edge of a fire spreading in a fuel bed of excelsior. Several experiments were done and the ROS values obtained with the visible cameras were compared with other results obtained using standard methods with a chronometer, thermocouples and photo-resistors. This comparison demonstrated the efficiency of the present method.
The experiments showed a dependence of the ROS with the fuel bed width. Two series of experiments with a fuel bed width varying between 0.25 m and 3.5 m were done in different environmental conditions. These experiments exhibited the same evolution for the rate of spread: an increase with the bed width up to an asymptotic value. The global evolution was well approximated with an exponential law involving two parameters. One parameter was found to be constant for this kind of experiment while the other depends on the environmental conditions (surrounding temperature and humidity).
A simulation was conducted based on a cellular automaton. Only radiative transfer was considered as the heat transfer leading to the fire spread. Radiative transfer between two cells was modeled with view factors between flames represented as cylinders above the burning cells and the surface of a “raw vegetation” cell.
Numerical results showed that the parabolic shape of the fire front is well captured. The evolution of the normalized numerical ROS with the fuel bed width was also found in agreement with the experimental results.
Future work will now extend this fire propagation model in considering the effect of slope or/and wind on the fire propagation in including a convective heat transfer contribution.

6. References

[1] M.A. Finney. FARSITE: Fire Area Simulator - model development and evaluation. Research Paper RMRS-RP-4. Ogden, UT: USDA Forest Service, Rocky Mountain Research Station. 47 p, 2004.
[2] P.L.Andrews. BehavePlus fire modeling system: Past, present, and future. In ‘Proceedings of 7th Symposium on Fire and Forest Meteorological Society’. 23-25 October 2007, Bar Harbor, Maine.

[3] G. Caldarelli, R. Frondoni, A. Gabrielli, M. Montuori, R. Retzkaff and C. Riccotta. Percolation in real wildfires. Europhys. Lett., Vol. 56 (4), pp. 510-516, 2001.
[4] H.E. Anderson. Fire spread and flame shape. J Fire Technology, Vol. 4, pp. 51-58, 1968.
[5] N. Otsu, A threshold selection method from gray-level histograms, IEEE Trans. Sys, Vol. 9, pp. 62-66, 1979.
[6] E. Pastor, A. Agueda, J. Andrade, M.A. Munoz, Y. Perez and E. Planas. Computing the rate of spread of linear flame fronts by thermal image processing. Fire Safety Journal, Vol. 41, pp. 569-579, 2006.
[7] W. R. Catchpole, E. A Catchpole, B. W. Butler, R. C. Rothermel, G. A. Morris and D. J. Latham, Rate of spread of free-burning fires in woody fuels in a wind tunnel, Combustion Science and Technology, Vol. 131, pp. 1-37, 1998.
[8] B. Porterie, N. Zekri, J.P. Clerc and J.C. Loraud. Influence of firebrands on wildland fire spread. Comptes Rendus de Physique, Vol. 6, pp. 1153-1160, 2005.